Russian Chemical Reviews **78** (12) 1123 – 1138 (2009) © 2009 Russian Academy of Sciences and Turpion Ltd

DOI 10.1070/RC2009v078n12ABEH004076

Synthesis of superheavy elements by cold fusion

S Hofmann

Contents

I.	Introduction	1123
II.	Nuclear structure and decay properties	1125
III.	Nuclear reactions	1130
IV.	Conclusion	1135

Abstract. The nuclear shell model predicts that the next doubly magic shell-closure beyond ^{208}Pb is at the proton number $Z = 114$, 120, or 126 and at the neutron number $N = 172$ or 184. The outstanding aim of experimental investigations is the exploration of this region of spherical 'Super Heavy Elements' (SHEs). Using cold fusion reactions which are based on lead and bismuth targets, the new elements from 107 to 112 were synthesized at GSI in Darmstadt, Germany. Some of these results were confirmed at RIKEN in Wako, Japan, where also a relatively neutron-deficient isotope of element 113 was synthesized. In hot fusion reactions of ^{48}Ca projectiles with actinide targets, a more neutron-rich isotope of element 112 and the new elements from 113 to 116 and even 118 were produced at FLNR in Dubna, Russia. Recently, part of these hot fusion data, which represent the first identification of nuclei located on the predicted island of SHEs, were confirmed in two independent experiments. The decay data reveal that for the heaviest elements, the dominant decay mode is α emission rather than fission. The decay properties as well as reaction cross-sections are compared with results of theoretical studies. The bibliography includes 120 references.

I. Introduction

Search for new elements is a journey into the unknown. The first scientifically based explorations were performed after the invention of the Periodic Table of the Elements by the Russian chemist D I Mendeleev and independently by the German chemist J L Meyer. At that time the aim was to fill the gaps still existing between the known elements. Although the element properties could be roughly estimated due to the periodic properties, deviations from the predicted chemical behaviour often hampered the discovery and assignment. However, such chemical properties slightly deviating from the expectation later yielded to unforeseen applications in the growing chemical industry.

Attempts to synthesize new elements beyond uranium started in the middle of the 1930s, when the atomic model was established and the constituents of the atomic nucleus were known. E Fermi and E Segrè in Rome and O Hahn and L Meitner in Berlin tried to use the nuclear reaction of neutron capture by uranium target nuclei and subsequent β decay for production of transuranium elements. Although most of the existing macroscopic quantities of transuranium elements up to einsteinium were produced later in nuclear reactors by this process, the discovery of Hahn and F W Strassmann [1] in 1938 was that uranium breaks into two approximately equal parts after neutron capture. This new phenomenon of nuclear fission was correctly described by Meitner and O R Frisch in 1939.[2] One year later, G N Flerov and K A Petrjak [3] detected that uranium decays also spontaneously by fission from its ground-state.

An appropriate description of the fission process was given by the charged liquid drop model. Using this model, binding energies could be calculated for a wide range of nuclei and an upper limit for the existence of nuclear matter was determined to be at element numbers of about 100 to 110.

The first new elements beyond uranium were synthesized during the years of the Second World War in laboratories in the US. These were the elements neptunium ($Z = 93$), plutonium (94), americium (95), and curium (96) (for details see *e.g.* G T Seaborg and W D Loveland [4]). In the years 1948 – 1955 the elements berkelium (97), californium (98), einsteinium (99), fermium (100), and mendelevium (101) were also produced in the US. The production processes were fusion with light ions like ^{2}H and ^{4}He, slow neutron capture in a nuclear reactor and subsequent β decay and for einsteinium and fermium, rapid neutron capture in a nuclear explosion and subsequent β decays.

Investigation of the chemical properties of these new elements was essential for the identification. These studies resulted in the concept of a second series of elements, the actinides, besides the known lanthanides, both having an

S Hofmann Gesellschaft für Schwerionenforschung (GSI), Helmholtzzentrum für Schwerionenforschung Gmbh, Planck-Str. 1, 64291 Darmstadt, Deutschland. Fax (49-061) 5971 29 02, Institut für Kernphysik der J W Goethe Universität, Max-von-Laue-Str. 1, 60438 Frankfurt am Main, Deutschland. Fax (49-069) 7984 71 00, tel. (49-061) 5971 27 34, e-mail: S.Hofmann@gsi.de

Received 13 May 2009
Uspekhi Khimii **78** (12) 1211 – 1227 (2009)

unfilled f-electron shell. In 1951 G T Seaborg and E M McMillan received the Nobel Prize in Chemistry for their studies on the synthesis and properties of transuranium elements.

Although the charged liquid drop model reproduces many collective properties of the nuclei very well, some known non-uniform structures demanded for a microscopic description. The increased binding energy of nuclei at the magic proton or neutron numbers 2, 8, 20, 28, 50 and 82 is the most obvious example. For neutrons, $N = 126$ was also identified as a magic number. However, the highest stability was observed in the case of the 'doubly magic' nuclei with a closed shell for both protons and neutrons. Amongst other special properties, the doubly magic nuclei are spherical and resist deformation.

In 1948 the magic numbers were successfully explained by the nuclear shell model,[5–7] and an extrapolation into unknown regions was thus undertaken. The numbers 126 for the protons and 184 for the neutrons were predicted to be the next shell closures. Instead of 126 for the protons also 114 or 120 were calculated as closed shells. The term superheavy elements (SHEs) was coined for these elements.

The perspectives offered by the nuclear shell model for production of SHEs and the need for developing more powerful accelerators for the synthesis of these elements in heavy ion fusion reactions were main motivations of Flerov for founding an own laboratory in 1957, which is now named after him, Flerov Laboratory of Nuclear Reactions, FLNR, one year after founding of the Joint Institute for Nuclear Research, JINR, in Dubna.

Studies of the elements 100 to 106 were performed with the new cyclotron U300 using fusion reactions with beams of ^{12}C to ^{22}Ne. In recognition of this early work in Dubna, element 105 is now officially named dubnium.

At approximately the same time the linear accelerator HILAC was constructed in Berkeley. The experiments there culminated in the synthesis of the new element 106. After careful investigation of discovery profiles by the International Unions of Pure and Applied Chemistry (IUPAC) and Physics (IUPAP), the names nobelium, lawrencium, and rutherfordium are now officially accepted for the elements 102, 103, and 104, respectively, as well as seaborgium for element 106.

Besides the synthesis of new elements and isotopes, the study of reaction mechanisms and nuclear structure was a main interest in early work at FLNR. The most important results are the discovery of fission isomers by S M Polikanov *et al.*,[8] the invention of cold fusion reactions for synthesis of SHEs by Yu Ts Oganessian *et al.*[9] and the detection and explanation of the break of systematically long half-lives of $N = 152$ isotope of element 104 due to the disappearance of a double humped fission barrier by Oganessian *et al.*[10]

In the mid-1960s the concept of the macroscopic-microscopic model for calculating binding energies of nuclei also at large deformations was invented by V M Strutinsky.[11] Using this method, a number of the measured phenomena could be naturally explained by considering the change in the binding energy as function of deformation. In particular it became possible to calculate the binding energy of a heavy fissioning nucleus at each point of the fission path and thus to determine the fission barrier.

Nevertheless, the calculation of the stability of SHEs against fission remained problematic. Predicted half-lives based on calculations using various parameter sets differed by many orders of magnitude.[12–18] Some of the half-lives approached the age of the universe, and attempts have been made to discover naturally occurring SHEs.[19,20] Although the corresponding discoveries were announced from time to time, none of them could be substantiated after more detailed inspection.

There was also great uncertainty on the production yields for SHEs. Closely related to the fission probability of SHEs in the ground state, the survival of the compound nuclei formed after complete fusion was difficult to predict. Even the best choice of the reaction mechanism, fusion or transfer of nucleons, was critically debated. However, as soon as relevant experiments could be performed, it turned out that the most successful methods for the laboratory synthesis of heavy elements are fusion – evaporation reactions using heavy-element targets, recoil-separation techniques, and the identification of the nuclei by generic ties to known daughter decays after implantation into position-sensitive detectors.[21–23]

The newly developed detection methods considerably extended the range of measurable half-lives. The lower half-life limit of about 1 μs is determined by the flight time through the separator. Long half-lives are measurable up to about one day. There, the limitation is given by the rate of implanted reaction products and background considerations. The detectors are sensitive for measuring all radioactive decays based on particle emission like proton radioactivity, α and β decay, and spontaneous fission (SF).

A further extension of the measuring possibilities was achieved with γ-ray, X-ray, or particle detectors mounted around the target. If these detectors are operated in delayed coincidence with signals from the implantation of reaction products and their radioactive decay in the focal plane of the separator, the sensitivity of 'in-beam' spectroscopy is significantly improved. This so called recoil decay tagging method was first applied in a study of the heavy ion radiative capture mechanism, a cold fusion process without any evaporation of nucleons,[24] using the reaction

$$^{90}\mathrm{Zr} + {}^{90}\mathrm{Zr} \longrightarrow {}^{180}\mathrm{Hg}.$$

Meanwhile, the method has become a standard tool in nuclear in-beam spectroscopy and it has become known as RDT method.

Detailed descriptions of the set-ups of the physics experiments used for the investigation of SHEs are given in review articles.[23,25,26] The chemistry methods used in recent discoveries of new isotopes in the heavy element region or in confirmation experiments were reported.[27–29] Cold and hot fusion reactions based on targets of lead or bismuth and isotopes of actinides, respectively, were used for the synthesis of SHEs. These experiments resulted in the identification of elements 107 to 112 (Ref. 23) at the Gesellschaft für Schwerionenforschung (GSI) in Darmstadt, Germany, in the confirmation of these data and in the production of a new isotope of element 113 (Refs 30–32) at the RIKEN laboratory in Wako, Japan, and in the synthesis of neutron-rich isotopes of element 112 and the production of the new elements from 113 to 116 and 118 (Ref. 33) at the Flerov Laboratory of Nuclear Reactions of the Joint Institute of Nuclear Research in Dubna, Russia. Recently, the results of two of these reactions, $^{48}\mathrm{Ca} + {}^{242}\mathrm{Pu}$ and $^{48}\mathrm{Ca} + {}^{238}\mathrm{U}$ were, confirmed in independent experiments.[29,34,35]

New isotopes were identified and confirmation experiments were performed [36,37] at the Lawrence Berkeley National Laboratory (LBNL) in Berkeley, USA. Results from in-beam spectroscopy experiments and experiments in the focal plane of separators were summarized.[38–40] Of great interest for such studies are isomeric states which are located in the regions of deformed heavy nuclei near $Z = 100$, $N = 152$ and $Z = 108$, $N = 162$. Figure 1 summarizes the data presently known in the region of SHEs.

The subsequent sections contain the results of theoretical descriptions of the properties of nuclei in the region of SHEs and phenomena that influence the yield for their synthesis. Empirical descriptions of hot and cold nuclear fusion reactions are outlined. Finally, a summary and an outlook are given.

II. Nuclear structure and decay properties

The calculation of the ground-state binding energy provides the basic step to determine the stability of SHEs. In macroscopic–microscopic models, the binding energy is calculated as the sum of a predominating macroscopic part (derived from the liquid-drop model of the atomic nucleus) and a microscopic part (derived from the nuclear shell model). In this way more accurate values for the binding energy are obtained than in the cases of using only the liquid drop model or the shell model. The shell correction energies of the ground state of nuclei near closed shells are negative, which results in further decreased values of the negative binding energy from the liquid drop model and, hence, increased stability. An experimental signature for the shell-correction energy is obtained by subtracting a calculated smooth macroscopic part from the measured total binding energy.

The shell-correction energy is plotted in Fig. 2*a* using data from Ref. 41. Two equally deep minima are obtained, one at $Z = 108$ and $N = 162$ for deformed nuclei with deformation parameters $\beta_2 \approx 0.22$, $\beta_4 \approx -0.07$ and the other one at $Z = 114$ and $N = 184$ for spherical SHEs. Different results are obtained from self-consistent Hartree–Fock–Bogoliubov calculations and relativistic mean-field models.[42–46] They predict, for spherical nuclei shells, $Z = 114$, 120, or 126 (indicated as dashed lines in Fig. 2*a*) and $N = 172$ or 184.

The knowledge of ground-state binding energies, however, is not sufficient for the calculation of partial SF half-lives. Here it is necessary to determine the size of the fission barrier over a wide range of deformation. The most accurate data have been obtained for even–even nuclei using a macroscopic–microscopic model.[47] Partial SF half-lives are plotted in Fig. 2*b*.[47,48]

The landscape of fission half-lives reflects the landscape of shell-correction energies, because in the region of SHEs, first, the height of the fission barrier is mainly determined by the ground-state shell correction energy, while the contribution from the macroscopic liquid-drop part approaches zero for $Z = 104$ and above, and, second, the shell correction energy at the saddle point is small.[49] Nevertheless the SF half-life is predicted to significantly increase from 10^3 s for deformed nuclei to 10^{12} s for spherical SHEs. This difference originates from an increasing width of the fission barrier when going from deformed to spherical nuclei.

Partial α half-lives decrease almost monotonically from 10^{12} s at $Z \approx 106$ down to 10^{-9} s near $Z = 126$ (Fig. 2*c*). However, as was pointed out,[48] non-smooth changes in Q_α values and associated half-lives can occur for some very proton-rich nuclei. Thus the calculated partial α half-life for $^{318}128$ is $10^{-8.15}$ s, whereas the half-life for $^{319}128$ is $> 10^{20}$ s. These extreme differences are due to multiple minima with extremely different quadrupole deformation in the potential energy surface.

The valley of β-stable nuclei passes through $Z = 114$, $N = 184$. At a distance of about 20 neutrons away from the bottom of this valley, β half-lives of isotopes have dropped down to values of one second (Fig. 2*d*).[48]

By combining results from the individual decay modes, one obtains the dominating partial half-life as shown in Fig. 3*a* for even–even nuclei. The two regions of deformed heavy nuclei near $N = 162$ and spherical SHEs merge and form a region of α emitters surrounded by spontaneously fissioning nuclei. The longest half-lives are 1000 s for deformed heavy nuclei and 30 years for spherical SHEs. It is interesting to note that the longest half-lives are not reached for the doubly magic nucleus 114 but for $Z = 110$ and $N = 182$. This is a result of continuously increasing Q_α values with increasing atomic number. Therefore, α decay becomes the dominant decay mode beyond darmstadtium with continuously decreasing half-lives. For nuclei at $N = 184$ and $Z < 110$ half-lives are determined by β^- decay.

The four-member α decay chain of $^{294}118$, the heaviest even–even nucleus, observed in a recent experiment in Dubna,[50] is also displayed in Fig. 3*a*. The arrows follow approximately the 1–10 ms contour line down to $^{282}112$. This is in agreement with the experimental observation. The nucleus $^{282}112$ is close to the region where theory predicts SF. The average values of the measured half-lives of the nuclei along the decay chain are 0.9 ms–7.1 ms–30 ms–0.82 ms, respectively. Only the predicted half-life of $^{286}114$ deviates from experiment by more than a factor of 10. However, this deviation is well within the accuracy limits of the calculation. Thus a change of the α energy of $^{286}114$ by 350 keV only changes the half-life by a factor of 10. Similar agreement with the half-life predictions exists for the decay chain of $^{292}116$ (Ref. 51).

The decay chain of ^{264}Hs (Refs 26, 52) and those of the two recently synthesized even–even nuclei, ^{270}Ds (Ref. 53) and ^{270}Hs (Ref. 54), are also shown in Figs 2 and 3. In these cases the decay chains end by SF at ^{256}Rf, ^{262}Sg, and ^{262}Rf, respectively.

For the odd nuclei displayed in Fig. 3*b*, the partial α and SF half-lives calculated in Ref. 41 have to be multiplied by a factor of 10 and 1000, respectively, thus making provisions for the odd particle hindrance factors. However, we have to keep in mind that fission hindrance factors show a wide variance from 10^1 to 10^5, which is mainly a result of the specific levels occupied by the odd nucleon.[55] For odd–odd nuclei, the fission hindrance factors from both the odd proton and the odd neutron have to be taken into account. For odd and odd–odd nuclei, the island character of α emitters disappears and for nuclei with neutron numbers 150 to 160, α decay prevails down to rutherfordium and beyond. In the allegorical representation where the stability of SHEs is seen as an island in a sea of instability, even–even nuclei portray the situation at high-tide and odd nuclei correspond to the low-tide, when the island is connected to the mainland.

Experimental shell-correction energies calculated as difference of binding energies from the liquid drop part of the macroscopic–microscopic models, *e.g.*, from Ref. 56

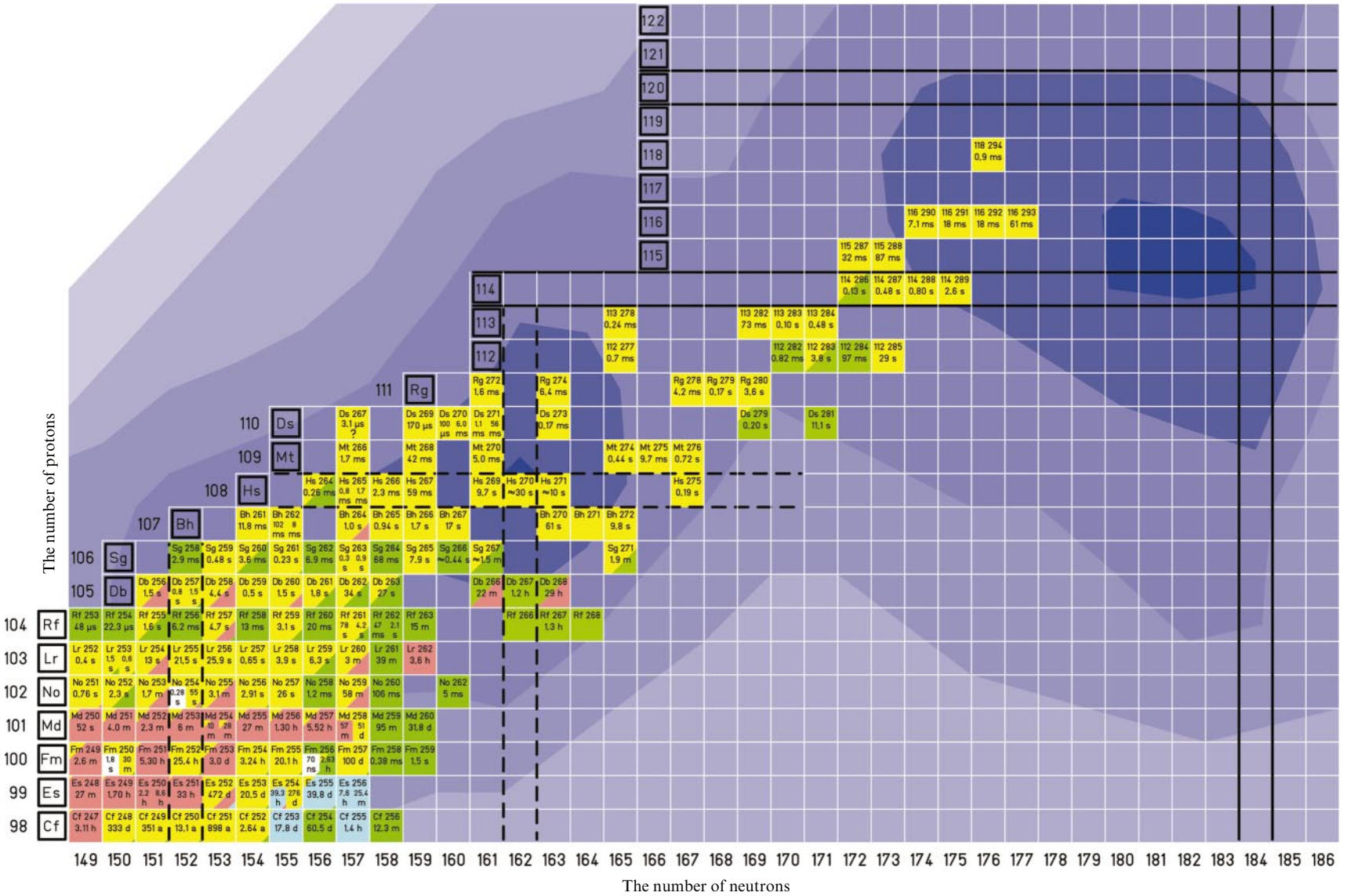


Figure 1. Upper end of the chart of nuclei showing the presently (2009) known nuclei. For each known isotope the element name, mass number, and half-life are given. The magic numbers for the protons at element 114 and 120 and for the neutrons at $N = 184$ are shown by bold lines. The dashed lines mark proton number 108 and neutron numbers 152 and 162. Nuclei with that number of protons or neutrons have increased stability, however, they are deformed contrary to the spherical superheavy nuclei. The crossing at $Z = 114$ and $N = 162$ reflects the uncertainty, whether nuclei in that region are deformed or spherical. The background structure shows the calculated shell correction energy according to the macroscopic–microscopic model (the higher the energy the darker the background).

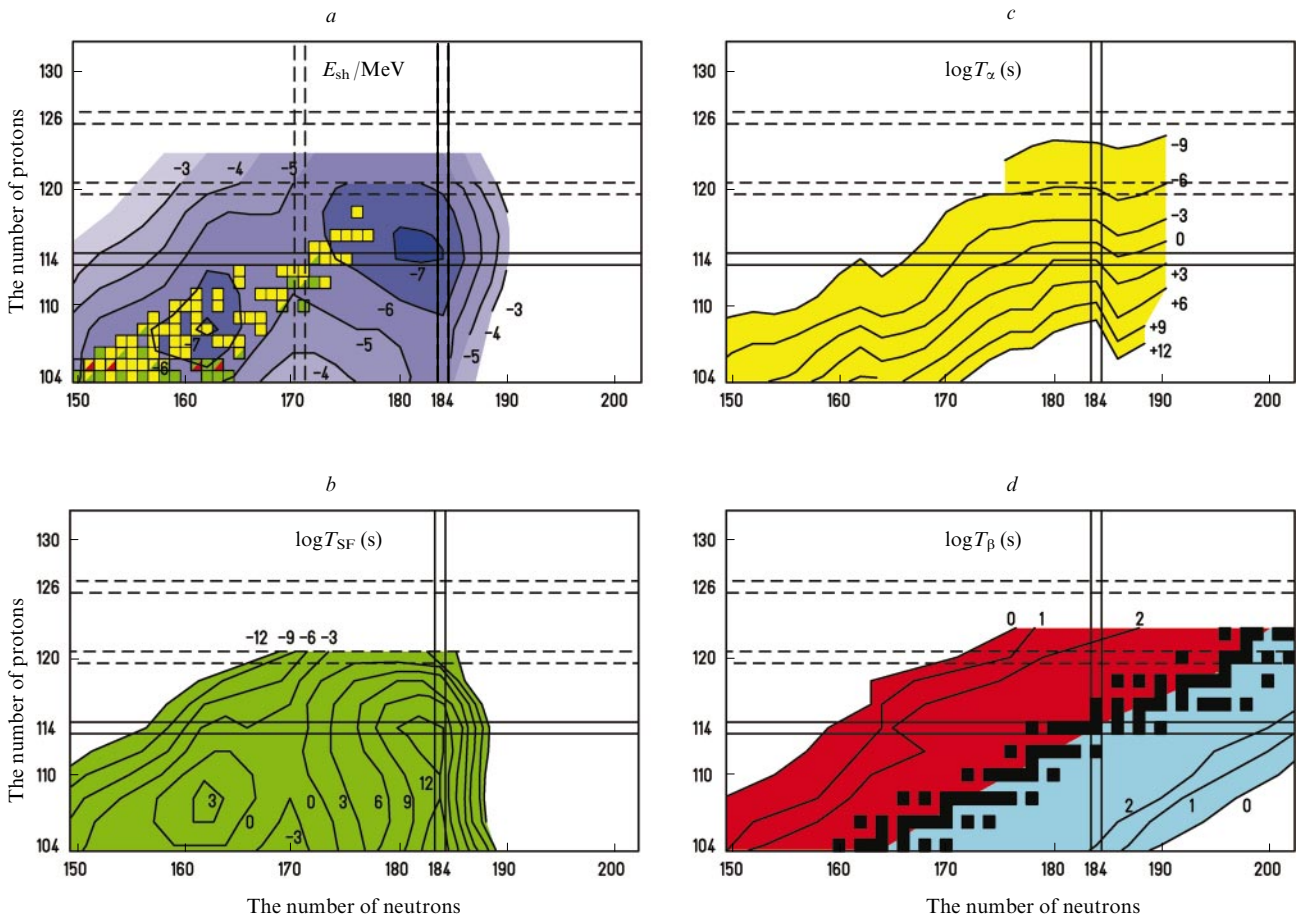


Figure 2. Shell-correction energy E_{sh} (*a*) [41] and partial half-lives for SF (*b*), α (*c*) and β decay (*d*). The light spots in (*a*) mark the nuclei presently known, the dark spots in (*d*) indicate the β stable nuclei.

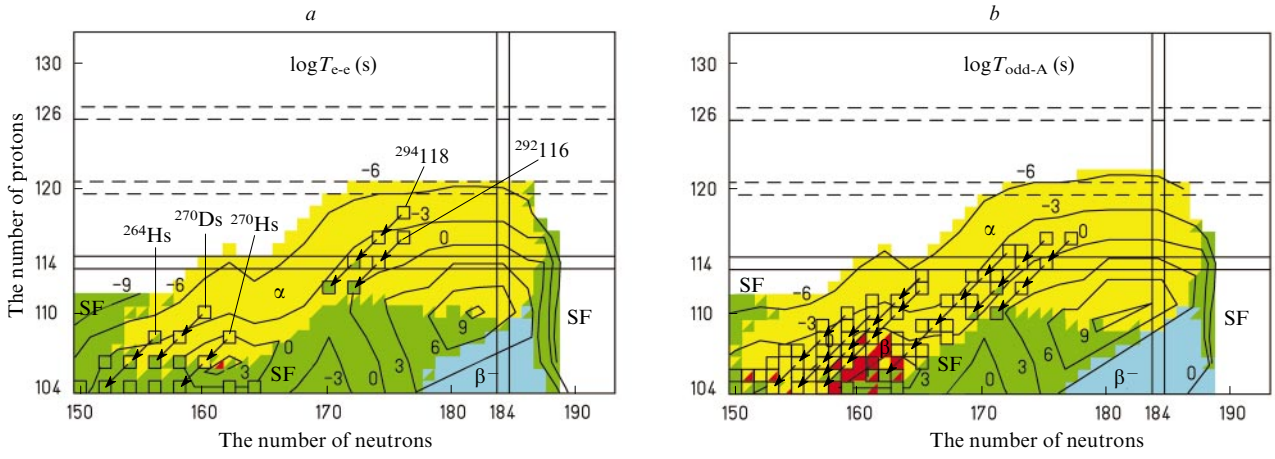


Figure 3. Dominating partial half-lives for α, β^+ and β^- decay and SF: (*a*) for even–even nuclei; (*b*) for odd-A nuclei. The currently known nuclei and decay chains are included.

and 57, and the measured binding energies cannot be determined for the new neutron-rich nuclei discovered in Dubna, because the endpoints of the α decay chains are not connected to known nuclei. However, it is possible to extract a trend of shell correction energies for nuclei along the measured decay chains by normalizing the binding energies to theoretical values at the end points. These nuclei are located close to the region of nuclei with known masses, where a good agreement between experimental and theoretical binding energies was observed. In Fig. 4 the data are plotted for the four chains starting at ^{288}115, ^{291}116, ^{293}116, and ^{294}118. The theoretical values were taken from Ref. 56.

The 'experimental' data deduced in this way reveal a monotonic decrease in the (negative) shell correction ener-

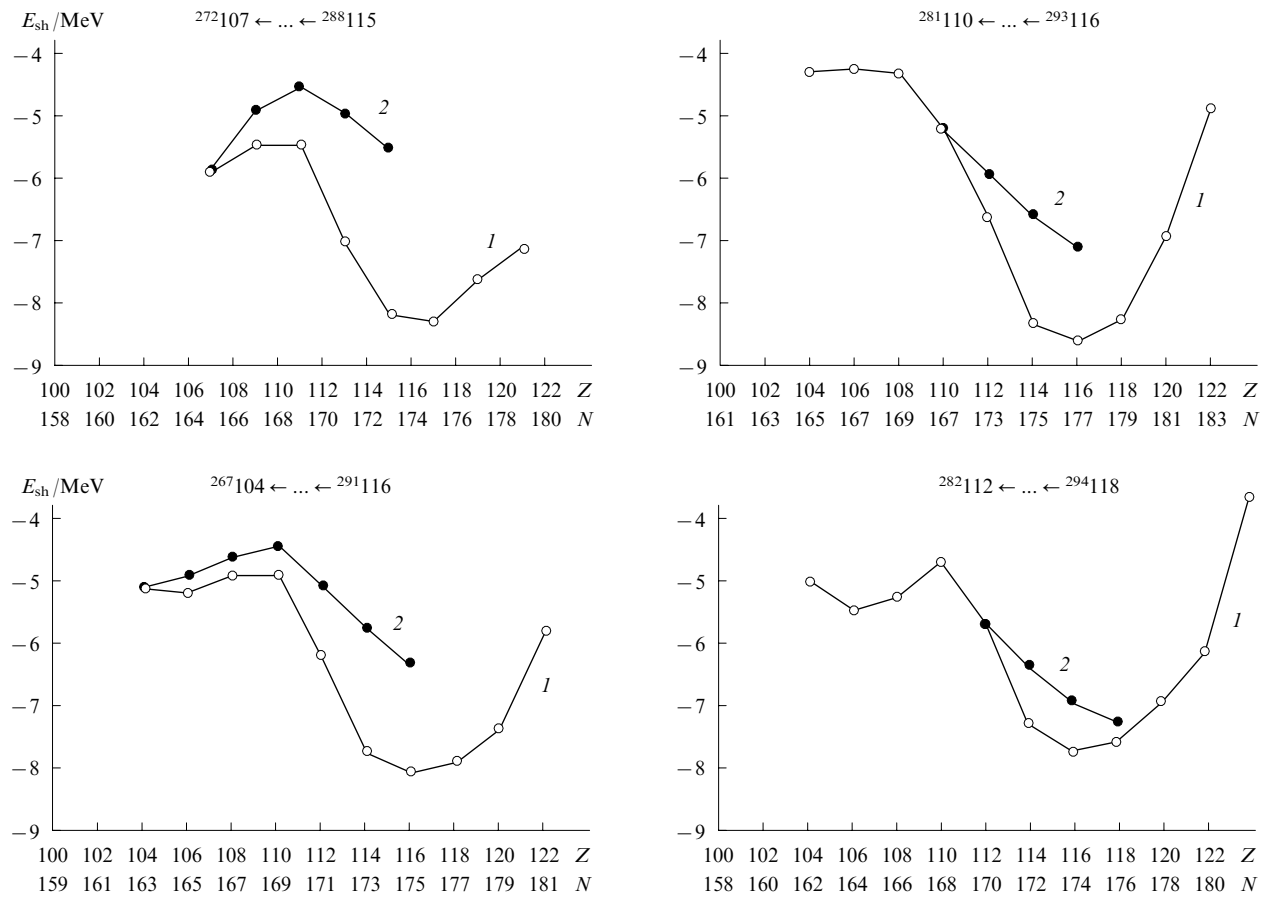


Figure 4. Comparison of calculated shell correction energies (curve *1*) [56] with 'experimental' ones (curve *2*) obtained as difference between calculated liquid drop binding energy taken from Ref. 56 and 'experimental' total binding energy obtained by using the measured Q_α values of nuclei along a decay chain.[33] The unknown shell correction energy of the nucleus at the end of a chain is normalized to the theoretical value.

gies when neutron number 184 is approached. No discontinuity is observed when the predicted closed shell at proton number 114 is crossed at neutron numbers 172 to 176. This result could mean that proton number 114 as a closed shell or subshell has less influence on the stability of SHEs than the closed neutron shell at $N = 184$. When planning future experimental work, this aspect should be taken into account.

The aim will be to reach $N = 184$, which is possible in various reactions using actinide targets and the neutron-richest, but still stable projectiles. These reactions lead into a region of elements as heavy as $Z = 120$ and beyond, where, however, increasing destructive Coulomb effects could further reduce half-lives and cross-sections. If, however, the predicted subshell closure at $Z = 120$ has a stronger influence on the stability of SHEs than the subshell closure at $Z = 114$, isotopes near $Z = 120$ and $N = 184$ might gain from increased stability and thus become accessible to experimental studies. These considerations are supported by results from recent theoretical investigations based on self-consistent nuclear models, which obtain increased stability for nuclei in the region of $Z = 120$ and $N = 184$ with certain parameter sets for the nuclear forces.[43,45] Nevertheless, various theoretical models predict different shell-correction energies of nuclei in this region, which cover a range from -6 MeV to -12 MeV, see *e.g.* Ref. 45 and references cited therein.

In order to probe the strength of the predicted closed neutron shell at $N = 184$ and that of a subshell closure at $Z = 120$, an experiment was planned and performed at SHIP [58] to search for element 120 using the reaction

$$^{64}\mathrm{Ni} + {}^{238}\mathrm{U} \longrightarrow {}^{302}120^{*}.$$

The irradiations were performed in three periods in 2007 and 2008. In the main part of the experiment, a cross-section limit of 90 fb was reached during a total beam time of 116 days. The chosen beam energy resulted in a mean excitation energy of 36.4 MeV where the cross-section maximum is expected.

Using a shell-correction energy of -7.0 MeV for the isotopes $^{299-302}120$, which converts into a fission-barrier height of $+7.0$ MeV, a cross-section of 4.5 fb was obtained for the reaction

$$^{64}\mathrm{Ni} + {}^{238}\mathrm{U} \longrightarrow {}^{299}120 + 3\mathrm{n}$$

in a recent theoretical study,[59] see Fig. 5. However, using the rule of thumb stating that a change of the fission barrier (BF) by 1 MeV results in a change of the cross-section by one order of magnitude, we would obtain a cross-section of 4.5 pb at a fission-barrier height of 10 MeV, leaving the probabilities for capture in the entrance channel and formation of the compound nucleus unchanged.

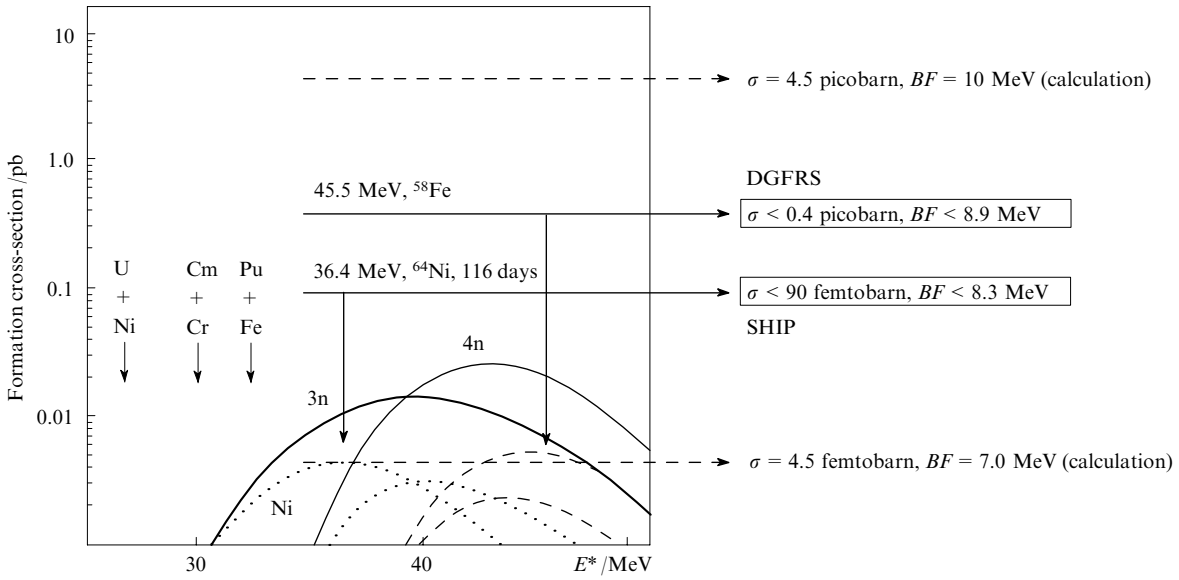


Figure 5. Calculated excitation functions for production of element $Z = 120$ in 3n and 4n evaporation channels of the fusion reactions $^{54}Cr + {}^{248}Cm$ (solid curves), $^{58}Fe + {}^{244}Pu$ (dashed lines), and $^{64}Ni + {}^{238}U$ (dotted lines). The corresponding Bass barriers [61] are marked by arrows. (Some parts of the figure were taken from Ref. 59).

The measured cross-section limit converts into a lower limit of the negative shell-correction energies of the isotopes $^{299-302}120$ of -8.3 MeV using the estimation as described before. Unusual large shell-correction energies at $Z = 120$ and $N = 184$ thus can be excluded.

In Dubna, a similar attempt to produce element $Z = 120$ was undertaken [60] using the reaction $^{58}Fe + {}^{244}Pu$, which results in the same compound nucleus $^{302}120^*$. In this experiment using gas-filled recoil separator (DGFRS), a cross-section limit of 400 fb was reached, which can be converted into a lower limit of -8.9 MeV of the shell correction energies. The experimental limits reached at the DGFRS and SHIP setups for cross-sections and deduced shell-correction energies and, correspondingly, fission barriers are plotted in Fig. 5. Also included are the excitation functions calculated [59] for three possible reactions resulting in one and the same compound nucleus $^{302}120^*$.

The most promising reaction for the synthesis of element $Z = 120$ is $^{54}Cr + {}^{248}Cm$. This is also the most asymmetric one, for which the lowest probability for re-separation of the reaction fragments in the entrance channel can be expected. Therefore as a main activity of the continuation of experimental studies on the synthesis and properties of superheavy elements at SHIP it is planned to systematically investigate hot fusion reactions based on ^{248}Cm targets. A first challenge will be the measurement of an excitation function for the synthesis of element 116 in the reaction $^{48}Ca + {}^{248}Cm$. This experiment will serve as a preparation for the study of $^{54}Cr + {}^{248}Cm$ and would result in another important confirmation of data measured in Ref. 51.

Two questions that had remained unanswered for a long time were recently tackled experimentally. Which is the maximum angular momentum that heavy nuclei can bear during the formation process and what is the degree of deformation in the ground state? The observation of high-spin states ($I \geqslant 10$) gives information on the fission barrier of heavy nuclei at high angular momentum. This information is important for understanding of the mechanism of the synthesis, since the fission barrier governs the survival probability. In fact, it is *a priori* not obvious that high-spin states of shell-stabilized nuclei will even survive against fission. Secondly, the stability of a large fraction of the isotopes that have so far been discovered for elements beyond fermium is predicted to arise from the ability of the nucleus to deform. However, a direct proof and a measurement of the degree of deformation were still missing.

The standard method for identifying high-spin states is in-beam gamma spectroscopy, but it is rarely used for studying very heavy nuclei because of the overwhelming fission background. This problem was overcome in recent experiments at the Argonne superconducting linear accelerator ATLAS and at the cyclotron of the University of Jyväskylä by using the RDT technique.[62–64]

The first reaction studied was

$$^{48}Ca + {}^{208}Pb \longrightarrow {}^{254}No + 2n,$$

which has a relatively high cross-section of 3 μb. The important result was the observation of the ground-state rotational band up to spin 18. The experiments demonstrated that shell effects stabilize heavy nuclei up to such high spin values and that ^{254}No is indeed a deformed nucleus. From the energies of the transitions, a quadrupole deformation parameter $\beta_2 = 0.27 \pm 0.02$ was deduced, which is in excellent agreement with theoretical predictions.[42, 43, 56, 65–70] The nucleus ^{254}No is a prolate spheroid with an axis ratio of 4 : 3. A review on more recent in-beam studies of rotational bands of nuclei in the region of ^{252}No was published.[40]

The reason for the increased stability of nuclei near $Z = 100$, $N = 152$ and also at $Z = 108$, $N = 162$ is the depression of single-particle Nilsson levels at relatively large prolate deformation, for both protons and neutrons, which results in large energy gaps above the compressed levels. Nuclei with Fermi levels below, within or slightly

above the gaps profit from the increased number of nucleons at lower negative binding energy, which results in the increased stability.

If the Fermi level is located within a band of close lying levels and levels of both high and low spin exist, relatively low-lying high- or low-spin K isomers can be formed. Detailed knowledge of the spectroscopic properties of these levels is particularly interesting since levels relevant for the location of the shell closures in the region of spherical SHEs could be involved.

Experimentally, the first K isomers in the region of interest were measured back 36 years ago.[71] These were the $T_{1/2} = 1.8$ s isomer in ^{250}Fm and the 0.28 s isomer in ^{254}No. A revival of more detailed studies of isomeric states in the region of heavy elements started in 2001 with the observation of a $T_{1/2} = 6.0$ ms isomer in ^{270}Ds at an energy of 1.13 MeV and its interpretation as a K isomer.[53] For the deformation of this nucleus the level gaps at $Z = 108$ and $N = 162$ at deformations of $\beta_2 = 0.23$ and $\beta_4 = -0.07$ are responsible. Single particle energies in the region of interest were calculated, using *e.g.*, the macroscopic–microscopic model[65,68] or a self-consistent mean field approach.[46] Extensive theoretical studies of K isomers in the region of heavy and superheavy elements were published.[72,73] Recently, experiments were performed for detailed investigation of K isomers in ^{254}No, ^{252}No, ^{250}Fm, and ^{256}Fm.[74–78]

Another source of information on the nuclear structure is investigation of binding energies using high precision mass measurements.[79] In recent years the range of Penning trap mass spectrometry has been extended towards more and more exotic nuclei by new technologies such as gas stopping of reaction products from fusion–evaporation reactions and fast beam fragmentation in combination with radiofrequency quadrupole beam coolers for beam preparation. The very high mass resolving power of Penning traps suffices to resolve isomeric states and results in an unmatched accuracy for the mass determination. It can now be applied to rare isotopes of nearly all elements. With the Penning trap mass spectrometer SHIPtrap at GSI, elements even above $Z = 100$ are accessible.

Since 2005, SHIPtrap has achieved high-precision mass measurements of about 60 rare isotopes contributing to nuclear astrophysics[80] and allowing for the first time an unambiguous determination of the proton drip line *via* direct mass measurements of proton-unbound nuclei.[81] In 2008, high-precision mass measurements of the nobelium isotopes $^{252-254}$No have been performed with SHIPtrap. A cyclotron resonance of ^{253}No is shown in Fig. 6. These experiments are the first direct mass measurements in the region above uranium.

Previously, the masses of ^{252,254}No were determined from Q_α measurements, whereas the ^{253}No mass was only known from extrapolations of systematic trends.[82] The experiments were very challenging due to the low production rates. Since ^{253}No has a production cross-section of about 400 nb in the reaction

$$^{48}\mathrm{Ca} + {}^{206}\mathrm{Pb} \longrightarrow {}^{252}\mathrm{No} + 3\mathrm{n}$$

at 4.55 A MeV, less than one ion per second was entering the SHIPtrap stopping cell. Mainly doubly charged nobelium ions were extracted from the stopping cell due to its high cleanliness, the low ionization rate by the incident ion beam, and an extraction time of a few milliseconds. The

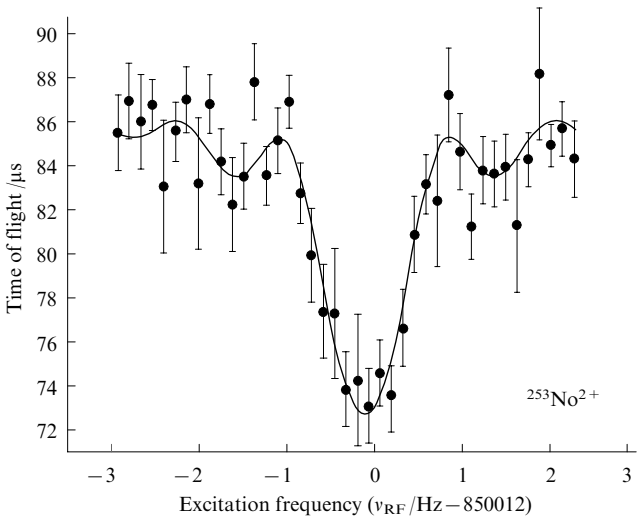


Figure 6. Cyclotron resonance of $^{253}No^{2+}$. The line represents a fit of the theoretical line shape to the experimental data points.

new, directly measured nobelium masses provide reference points in this mass region and can be used to accurately determine the masses of heavier nuclei up to darmstadtium ($Z = 110$) using α-decay links.

III. Nuclear reactions

The main features which determine the fusion process of heavy ions are

(1) the fusion barrier and the related beam energy and excitation energy,

(2) the ratio of surface tension *versus* Coulomb repulsion which determines the fusion probability and which strongly depends on the asymmetry of the reaction partners (the product $Z_1 \times Z_2$ at fixed $Z_1 + Z_2$),

(3) the impact parameter (centrality of collision) and related angular momentum, and

(4) the ratio of neutron evaporation and gamma emission *versus* the fission of the compound nucleus.

In fusion reactions towards SHEs the product $Z_1 \times Z_2$ reaches extremely large and the fission barrier extremely small values. In addition, the fission barrier itself is fragile, because it is solely built up from shell effects (see Section 2). For these reasons the fusion of SHEs is hampered twofold: (1) in the entrance channel by a high probability for reseparation and (2) in the exit channel by a high probability for fission. In contrast, the fusion of lighter elements proceeds unhindered through the contracting effect of the surface tension and the evaporation of neutrons instead of fission.

Cross-section data obtained in reactions for production of heavy elements are plotted in Fig. 7. The 1n and 2n reactions with ^{208}Pb and ^{209}Bi targets result from low excitation energies of about 10–15 and 15–25 MeV, respectively, (therefore named cold fusion) whereas reactions with actinide targets yield excitation energies of 35–45 MeV (hot fusion) with the 3n and 4n channels being particular interesting. The lowest cross-section value was measured to be 31 fb for the production of element 113 in cold fusion.[31,32] This is the extreme limit presently set by experimental constraints. Considering the already long irradiation time of about 2 weeks to reach a cross-section

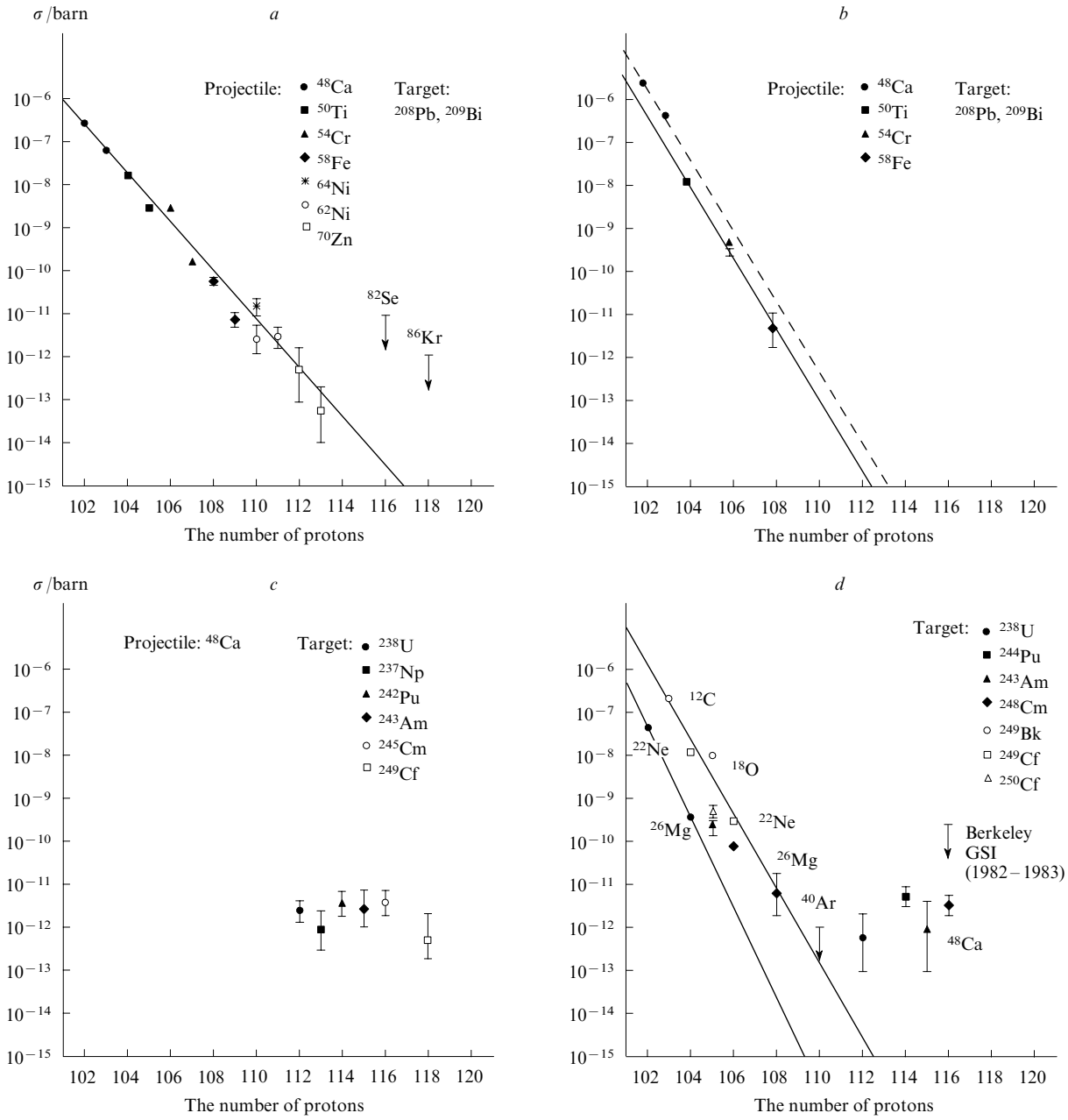


Figure 7. Measured cross-sections for fusion reactions with ^{208}Pb and ^{209}Bi targets (*a*, *b*) with evaporation of one [*a*, 1n channel, $E^* = 10-15$ MeV, $(N-Z)/2 = 3$] and two [*b*, 2n channel, $E^* = 20-25$ MeV, $(N-Z)/2 = 3$] neutrons and for fusion reactions with actinide targets (*c*, *d*) with evaporation of three [*c*, 3n channel, $E^* = 35-40$ MeV, $(N-Z)/2 = 4$] and four neutrons (*d*, 4n channel, $E^* = 40-45$ MeV, $(N-Z)/2 = 1$). The values $(N-Z)/2$ characterize the neutron excess of the projectile.

of 1 pb, it seems difficult to perform systematic studies at this cross-section level or even below. Further improvement of the experimental conditions is mandatory. Note in this context that the experimental sensitivity increased by three orders of magnitude since the 1982–1983 LBNL–GSI search experiment for element 116 using a hot fusion reaction,[83] see Fig. 7 *d*.

The cross-sections for elements up to 113 decrease by a factor of 4 per element in the case of cold fusion (1n channel) and those for elements lighter than 110 by a factor of 10 in the case of hot fusion (4n channel). The decrease is explained as a combined effect of increasing probability for re-separation of projectile and target like nuclei in the entrance channel of the reaction and fission of the compound nucleus in the exit channel. Theoretical considerations and studies (see *e.g.* Refs 23, 26, 84–89) suggest that the steep decrease of cross-sections for cold fusion reactions with increasing Z may be strongly linked to increasing re-separation probability at high values of $Z_1 \times Z_2$ while hot fusion cross-sections mainly drop because of strong fission

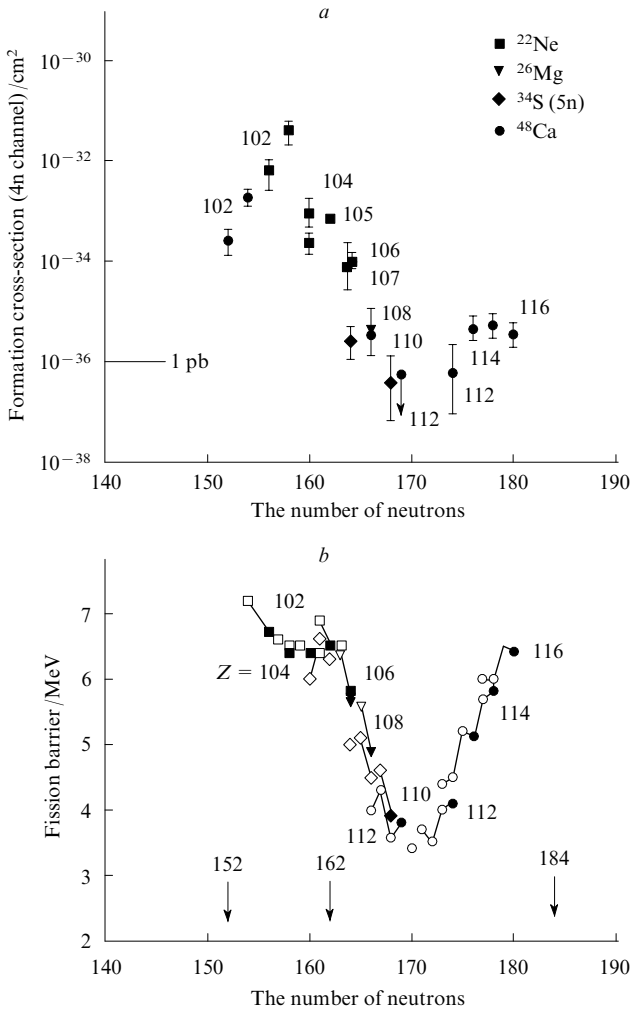


Figure 8. Measured cross-sections of hot fusion reactions to form nuclei with $Z \geqslant 102$ (*a*) and calculated fission barriers[47,90] (*b*), revealing the mutual relation between these two quantities (see text for details). The figure is taken from Ref. 51.

losses at high excitation energies and decreasing fission barrier already in the ground-state.

Extremely small cross-section values result from extrapolation of these data into the region of element 114 and beyond. However, the experimental data in the case of hot fusion reveal an opposite trend. The cross-sections increase again and reach maximum values of about 3 pb at element 114 and 116 for both 3n and 4n evaporation channels, Figs 7 *c*, *d*. Only relatively high cross-section limits exist for element 116 and 118 in the case of cold fusion, Fig. 7 *a*.

The relationship between measured cross-sections and calculated fission barriers[47,90] is plotted in Fig. 8. As discussed before, cross-sections and fission barriers decrease up to element 110, and on further increase in Z, both values increase again. The reason for the fact that the cross-sections increase to a lesser extent than the fission barriers could be that the latter quantities are actually smaller than predicted or, which seems more likely, that increasing

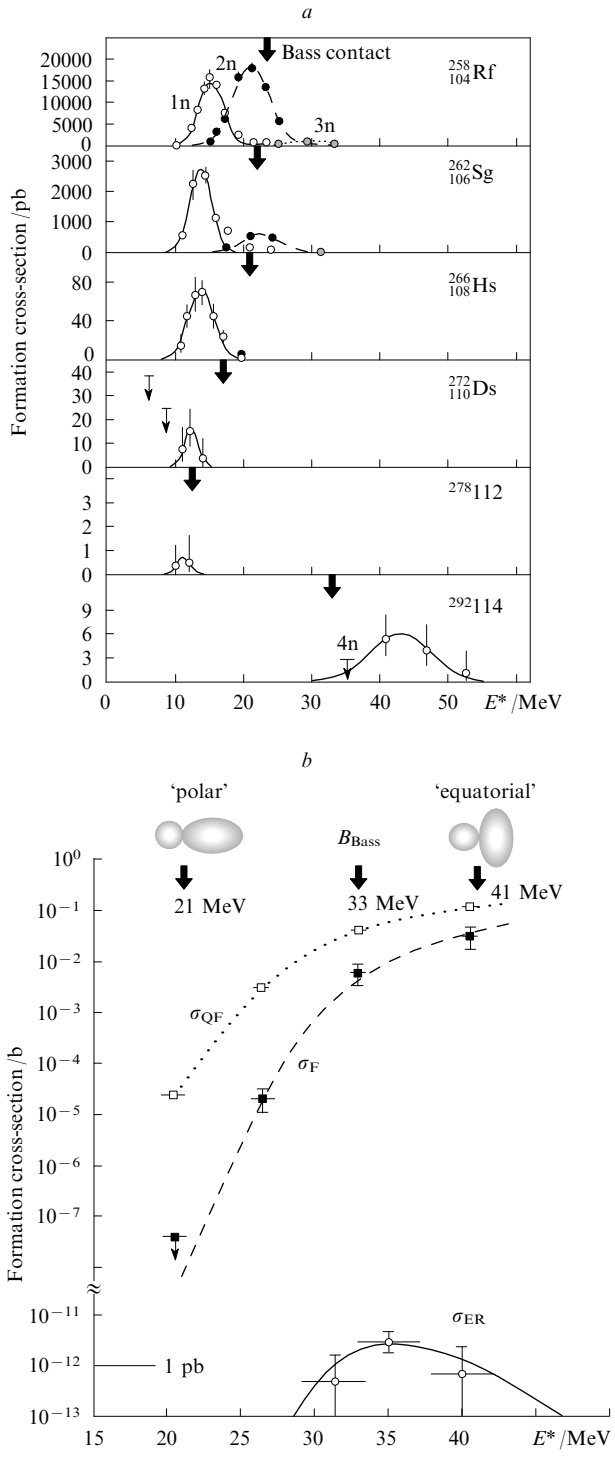


Figure 9. (*a*) Excitation functions of even elements from rutherfordium to element 112 produced in reactions with ^{208}Pb targets and beams from ^{50}Ti to ^{70}Zn measured in experiments at SHIP. For comparison, the excitation function for synthesis of element 114 in the reaction ^{48}Ca + ^{244}Pu is also plotted.[51] The arrows mark the energy at reaching a contact configuration using the model by Bass.[61]
(*b*) Cross-sections as functions of the excitation energy E^* for quasi-fission (QF), compound fission (F), and evaporation residues (ER) for the reaction ^{48}Ca + ^{238}U. Figure 9 *b* is taken from Ref. 51.

Coulomb repulsion in the entrance channel leads to a reduced fusion probability.

A number of excitation functions was measured for the synthesis of elements from nobelium to darmstadtium using cold fusion reactions based on lead and bismuth targets.[23] For the even elements these data are shown together with the two data points measured for the compound nucleus ^{278}112 in Fig. 9. The maximum evaporation residue cross-section (1n channel) was measured at beam energies well below a one dimensional fusion barrier.[61] At the optimum beam energy, projectile and target are just reaching the contact configuration in a central collision. The relatively simple fusion barrier based on the Bass model[61] is too high and a tunnelling process through this barrier cannot explain the measured cross-section. Various processes may result in a lowering of the fusion barrier. Among these processes transfer of nucleons and an excitation of vibrational degrees of freedom are most important.[91–94]

The target nuclei of actinide targets are strongly deformed and the height of the Coulomb barrier depends on the orientation of the deformation axes. Two of the measured excitation functions for production of ^{292}114 and ^{283}112 (Ref. 51) after evaporation of four and three neutrons, respectively, are shown in Fig. 9*a*. A comparison with the cold fusion data reveals that the element 114 excitation function is located completely above the Bass contact configuration which was calculated for a mean radius of the deformed target nucleus. In addition, the curves for the hot fusion reactions are significantly broader, *e.g.*, 10.6 instead of 4.6 MeV (FWHM) as measured for ^{265}Hs.

Figure 9*b* compares the fusion evaporation excitation function with the yield of quasi-fission and compound nucleus fission.[95] At low projectile energies nuclear reactions can occur only at polar orientation of the deformed target nucleus. In the upper part of the Figure the orientation at the touching point and the corresponding Coulomb energy are indicated. Although the excitation energy of the compound nucleus would be low, about 20–25 MeV resulting in reduced fission of the compound nucleus, the nuclei do not fuse but re-separate with high probability at this elongated configuration. Only the compact configuration in the case of near equatorial collisions results in fusion despite the fact that the compound nucleus is considerably higher excited, about 35–40 MeV.

It was pointed out in the literature[96–98] that closed shell projectile and target nuclei are preferable for synthesizing SHEs. The reason is not only a low (negative) reaction *Q*-value and thus a low excitation energy, but also the fact that fusion of such systems is connected with a minimum of energy dissipation. The fusion path proceeds along cold fusion valleys, where the reaction partners maintain kinetic energy up to the closest possible distance. In the case of cold fusion with spherical targets the maximum fusion yield is obtained at projectile energies just sufficiently high for the projectile and target nucleus to come to rest when just the outer orbits are in contact.

Figure 10 (see p. 1135) shows centre of mass energy-*vs*-distance diagram for the reaction of an almost spherical ^{64}Ni projectile with a spherical ^{208}Pb target nucleus resulting in the deformed fusion product ^{271}110 after emission of one neutron. At the centre-of-mass energy of 236.2 MeV, the maximum cross-section was measured. Figure 10*a* shows the reaction partners represented by their nuclear potentials (Woods–Saxon) at the contact configuration where the initial kinetic energy is exhausted by the Coulomb potential. At this configuration projectile and target nuclei are 14 fm apart from each other. This distance is 2 fm larger than the Bass contact configuration,[61] where the mean radii of projectile and target nucleus are in contact. In Fig. 10*b*, the outermost proton orbitals are shown at the contact point. For the projectile ^{64}Ni, an occupied $1f_{7/2}$ orbit is drawn, and for the target ^{208}Pb an empty $1h_{9/2}$ orbit is drawn. Empty orbits above the closed shell nucleus ^{208}Pb favour a transfer of nucleons from the projectile to the target and thus initiate the fusion process. The Coulomb repulsion, and thus the probability for separation, is reduced by the transfer of protons. Then fusion occurs easily along the path of minimum energy dissipation. An adequate theoretical description of this process is given by the application of the two-centre shell model.[99–102]

At the first glance the situation seems to be different in the case of hot fusion. The maximum of the excitation function is located at the higher energy side of the value needed to reach the contact configuration according to the Bass model,[61] see Fig. 9. However, taking into account the deformation of the target nucleus and considering fusion at near equatorial orientation, it is evident that the projectile and target nuclei come to rest when just the outer orbits are in contact. This distance corresponds to the energy, where the maximum yield is measured. For an accurate calculation, the relatively large hexadecapole deformation of the target nucleus has to be considered, which results in a closest approach slightly off a central equatorial collision, see Fig. 11 (p. 1135). Also in this case the empty orbits in the near equatorial plane of the prolate deformed target nucleus favour the transfer of nucleons. Theoretical investigations taking into account the deformation of the reaction partners are presented in Refs 103–106.

At low projectile energies, where a contact configuration at zero kinetic energy in the centre of mass system is reached only in polar collisions, the nuclei do not fuse. The reasons are, firstly, that at the elongated configuration re-separation is enhanced due to the unfavourable ratio of Coulomb repulsion and surface attraction and, secondly, due to the occupied Nilsson levels originating from orbits of high spin in the target nucleus, which hinders a transfer of nucleons from the projectile to the target. Recent experimental work is aiming to study the transition from fusion with deformed actinide target nuclei and light projectiles, *e.g.* ^{12}C or ^{16}O, where polar collisions at low beam energy result in enhanced sub-barrier fusion, to heavier projectiles like ^{48}Ca just described, as function of the projectile mass and charge.[107]

Figure 12 (see p. 1135) illustrates the two different scenarios of the ^{48}Ca + ^{248}Cm reaction starting from an elongated (*a*) and a compact (*b*) configuration of the participating nuclei. For low projectile energy (Fig. 12*a*), the contact with the target nucleus can occur only at its polar orientation. When the projectile energy is high enough (Fig. 12*b*), the contact occurs also at equatorial orientation. In both cases the projectile energies are chosen so that the

kinetic energy in the centre of mass system is zero at the contact configuration.

Triggered by the recent experimental success of heavy element synthesis, a number of theoretical studies were performed or are in progress, aiming to obtain a detailed quantitative understanding of the reaction processes involved in heavy element synthesis.[89, 94, 106, 108 – 117]

Due to the great uncertainty concerning the influence of the various steps in the fusion of heavy nuclei, more and more precise experimental data are needed. It is especially important that various combinations of projectile and target be investigated, from very asymmetric systems to symmetric ones, studied for both fusion and transfer reactions, the latter for systems as heavy as $^{238}U + ^{248}Cm$ (Ref. 118) and that excitation functions are measured. This provides information on how fast the cross-section decreases with increasing energy due to fission of the compound nucleus and how fast cross-sections decrease on the low energy side due to the fusion barrier and re-separation of projectile and target nuclei. From both slopes, information about the shape of the fission and the fusion barriers can be obtained.

Investigation of transfer products at beam energies near and below the Coulomb barrier may open a direct access to the first steps of the processes resulting in fusion. Due to the low beam energy the reactions occur in central collisions and the reaction partners re-separate in and opposite to the beam direction. Therefore velocity separators like SHIP are an ideal tool to study these processes.[119] Similarly neutron rich heavy nuclei could be produced in transfer reactions as suggested in Ref. 118. Also in these cases low beam energies and hence observation in zero degree direction are mandatory, in order to produce the fragments at the lowest possible excitation energy and thus reducing fission of the fragments.

At a high enough cross-section, the measurements can be complemented by in-beam gamma-ray spectroscopy using the RDT method in order to study the influence of angular momentum on the fusion and survival probability.[120]

IV. Conclusion

The experimental work of the last three decades has shown that cross-sections for the synthesis of the heaviest elements do not decrease continuously as it was measured up to the production of element 112 using a cold fusion reaction. Recent data on the synthesis of elements 113 to 116 and 118 in Dubna using hot fusion break this trend when the region of spherical SHEs is reached. Some of the results originally obtained in Dubna were confirmed in independent experiments and with different methods, including the use of chemical, element specific properties. Due to the systematic study of different reactions for the production of SHEs and the measurement of excitation functions, the present assignment of the measured decay chains to new relatively neutron-rich isotopes of SHEs is highly reliable. The region of the predicted spherical SHEs has finally been reached and the exploration of the 'island' has started and can be performed even on a relatively high cross-section level.

The progress towards the exploration of the island of spherical SHEs is difficult to predict. However, despite the exciting new results, many questions of more general character are still awaiting an answer. New developments will not only make it possible to perform experiments aimed at synthesizing new elements in reasonable measuring times, but will also allow for a number of various other investigations covering reaction physics and spectroscopy.

One can hope that, during the coming years, more data will be measured in order to promote a better understanding of the stability of the heaviest elements taking into account the fundamental properties of the nuclear forces. A microscopic description of the fusion process will be needed for an effective explanation of all measured phenomena in the case of low dissipative energies. Then, the relationships between fusion probability and stability of the fusion products will result in accurate predictions of the production yield of SHEs using various reaction mechanisms.

An opportunity for the continuation of experiments in the region of SHEs at low cross-sections afford, among others, further accelerator developments. High current beams and radioactive beams are options for the future. At increased beam currents, values of tens of particle microampere may become accessible, the cross-section level for the performance of experiments can be shifted down into the region of tens of femtobarns, and excitation functions can be measured on the level of tenths of picobarns. High currents, in turn, call for the development of new targets and separator improvements. Radioactive ion beams, not as intense as the ones with stable isotopes, will allow for approaching the closed neutron shell $N = 184$ already at lighter elements. The study of the fusion process using radioactive neutron rich beams will be highly interesting.

The half-lives of spherical SHEs are expected to be relatively long. Based on nuclear models, which are effective predictors of half-lives in the region of the heaviest elements, values from microseconds to years have been calculated for various isotopes. This wide range of half-lives encourages the application of a wide variety of experimental methods in the investigation of SHEs, from the safe identification of short lived isotopes by recoil-separation techniques to atomic physics experiments on trapped ions, and to the investigation of chemical properties of SHEs using long-lived isotopes.

The nobelium mass measurements with SHIPtrap represent a major breakthrough in Penning trap mass spectrometry. Along with laser resonance ionization and trap-assisted decay spectroscopy they open up new perspectives for sensitive high precision studies of very heavy nuclei at low energy utilizing ion traps. In the near future, further technical improvements such as a cryogenic stopping cell, for example, will be implemented and the experimental program will be extended to even higher Z.

Finally, on the basis of a broader knowledge of the properties of SHEs and the mechanisms of their synthesis, it will become possible to answer reliably the questions whether or not SHEs could be produced in nature and where the highest probability may exist.

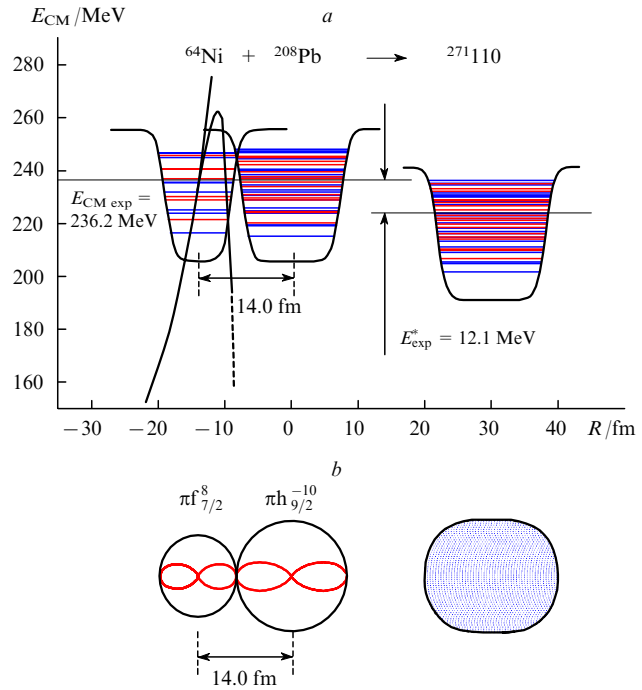


Figure 10. (*a*) Centre of mass energy-*vs*-distance diagram for cold fusion reaction of an almost spherical ^{64}Ni projectile with a spherical ^{208}Pb target nucleus resulting in the deformed fusion product ^{271}110 after emission of one neutron.
(*b*) Outermost proton orbitals at the contact point. For the projectile ^{64}Ni, an occupied $1f_{7/2}$ orbit is drawn, and for the target ^{208}Pb an empty $1h_{9/2}$ orbit. The protons circulate in a plane perpendicular to the drawing. (The Figure is taken from Ref. 93.)

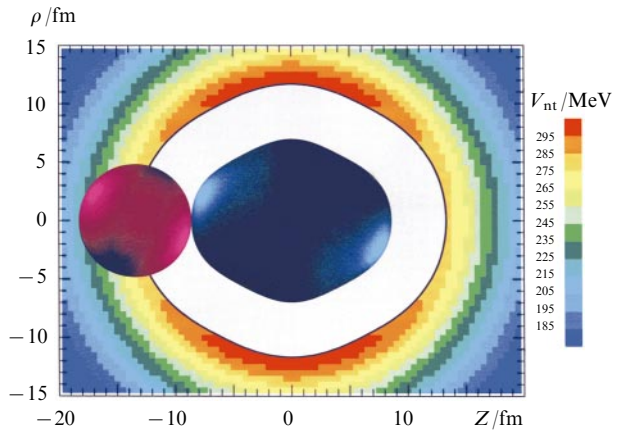


Figure 11. Coulomb potential between a deformed ^{238}U target nucleus and an almost spherical ^{70}Zn projectile resulting in the compound nucleus ^{308}122. The calculations were performed only up to the contact configuration. The figure was provided by P Möller, see also Refs 103 and 104.

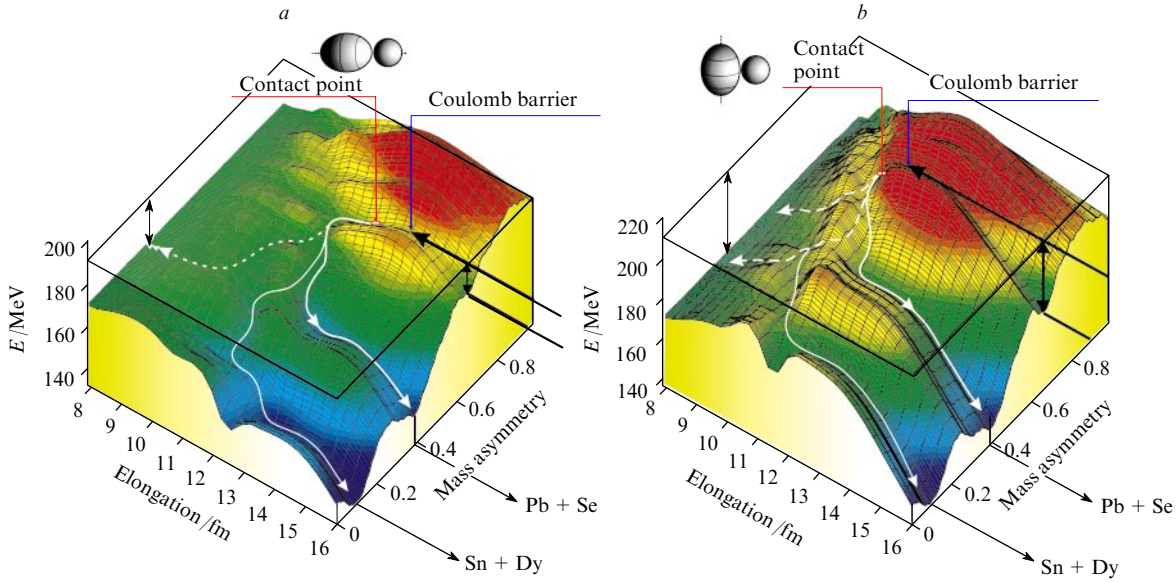


Figure 12. Three-dimensional potential energy surface as function of elongation and mass asymmetry for the reaction ^{48}Ca + ^{248}Cm for low (*a*) and sufficiently high (*b*) projectile energy. The rectangular plane (above) marks the total energy. The difference between this plane and the curved potential energy surface is mainly kinetic energy in the entrance channel (before the contact) or mainly intrinsic excitation energy of the system (after the contact). The valleys in the potential energy surface are due to shell effects of the reaction partners. After contact the paths of the configuration in the plane of total energy are influenced by the structure of the potential energy surface. Trajectories above the valleys are favoured due to enhanced conversion of potential energy into kinetic energy, which results in re-separation dominantly with the double magic ^{208}Pb as one of the reaction partners. For the elongated configuration (*a*), the probability for re-separation is higher due to the longer distance from contact to the compound system. Therefore, the fusion cross-section is considerably smaller as in the case of the compact configuration (*b*), although the excitation energy of the compound nucleus (marked by the length of the double arrow on the left) is significantly smaller (about 20 MeV instead of 40 MeV). The main part of the Figure has been provided by courtesy of V I Zagrebaev (2007).

References

1. O Hahn, F Strassmann *Naturwissenschaften* **27** 11 (1939)
2. L Meitner, O R Frisch *Nature (London)* **143** 239 (1939)
3. G N Flerov, K A Petrjak *Phys. Rev.* **58** 89 (1940)
4. G T Seaborg, W D Loveland *The Elements beyond Uranium* (New York: Wiley, 1990)
5. M G Mayer *Phys. Rev.* **74** 235 (1948)
6. O Haxel, J H D Jensen, H D Suess *Phys. Rev.* **75** 1769 (1949)
7. H Grawe *Lect. Notes Phys.* **651** 33 (2004)
8. S M Polikanov,V A Druin, V A Karnaukhov, V L Mikheev, A A Pleve, N K Skobelev, V G Subbotin, G M Ter-Akopyan, V A Fomichev *J. Exp. Theor. Phys.* **15** 1016 (1962)
9. Yu Ts Oganessian, A S Iljinov, A G Demin, S P Tretyakova *Nucl. Phys. A* **239** 353 (1975)
10. Yu Ts Oganessian, A G Demin, A S Iljinov, S P Tretyakova, A A Pleve, Yu E Penionzhkevich, M P Ivanov, Yu P Tretyakov *Nucl. Phys. A* **239** 157 (1975)
11. V M Strutinsky *Nucl. Phys. A* **95** 420 (1967)
12. W D Myers, W J Swiatecki *Nucl. Phys. A* **81** 1 (1966)
13. H Meldner *Ark. Fys.* **36** 593 (1967)
14. S G Nilsson, J R Nix, A Sobiczewski, Z Szymański, S Wycech, C Gustafson, P Möller *Nucl. Phys. A* **115** 545 (1968)
15. U Mosel, W Greiner *Z. Phys. A* **222** 261 (1969)
16. J Grumann, U Mosel, B Fink, W Greiner *Z. Phys. A* **228** 371 (1969)
17. E O Fiset, J R Nix *Nucl. Phys. A* **193** 647 (1972)
18. J Randrup, S E Larsson, P Möller, S G Nilsson, K Pomorski, A Sobiczewski *Phys. Rev. C* **13** 229 (1976)
19. W Grimm, G Herrmann, H-D Schüssler *Phys. Rev. Lett.* **26** 1040 (1971)
20. G N Flerov, G M Ter-Akopian *Rep. Prog. Phys.* **46** 817 (1983)
21. G Münzenberg, W Faust, S Hofmann, P Armbruster, K Güttner, H Ewald *Nucl. Instr. Meth.* **161** 65 (1979)
22. S Hofmann, W Faust, G Münzenberg, W Reisdorf, P Armbruster, K Güttner, H Ewald *Z. Phys. A* **291** 53 (1979)
23. S Hofmann, G Münzenberg *Rev. Mod. Phys.* **72** 733 (2000)
24. K-H Schmidt, R S Simon, J-G Keller, F P Heßberger, G Münzenberg, B Quint, H-G Clerc, W Schwab, U Gollerthan, C-C Sahm *Phys. Lett. B* **168** 39 (1986)
25. G Münzenberg, in *Flight Separation of Heavy Ion Beams in Experimental Techniques in Nuclear Physics* (Eds D N Poenaru, W Greiner) (Berlin: Walter de Gruyter, 1997) p. 375
26. S Hofmann *Rep. Prog. Phys.* **61** 639 (1998)
27. M Schädel *The Chemistry of Superheavy Elements* (Dordrecht: Kluwer Academic, 2003)
28. J V Kratz, in *Handbook of Nuclear Chemsitry* Vol. 2 (Eds A Vertes, S Nagy, Z Klencsar) (Dordrecht: Kluwer Academic, 2003) p. 323
29. R Eichler, N V Aksenov, A V Belozerov, G A Bozhikov, V I Chepigin, S N Dmitriev, R Dressler, H W Gäggeler, V A Gorshkov, F Haenssler, M G Itkis, A Laube, V Ya Lebedev, O N Malyshev, Yu Ts Oganessian, O V Petrushkin, D Piguet, P Rasmussen, S V Shishkin, A V Shutov, A I Svirikhin, E E Tereshatov, G K Vostokin, V Wegrzecki, A V Eremin *Nucl. Phys. A* **787** 373 (2007)
30. K Morita, K Morimoto, D Kaji, T Akiyama, S Goto, H Haba, E Ideguchi, K Katori, H Koura, H Kudo, T Ohnishi, A Ozawa, T Suda, K Sueki, F Tokanai, T Yamaguchi, A Yoneda, A Yoshida *J. Phys. Soc. Jpn.* **76** 043201 (2007)
31. K Morita, K Morimoto, D Kaji, T Akiyama, S Goto, H Haba, E Ideguchi, R Kanungo, K Katori, H Koura, H Kudo, T Ohnishi, A Ozawa, T Suda, K Sueki, H S Xu, T Yamaguchi, A Yoneda, A Yoshida, Y L Zhao *J. Phys. Soc. Jpn.* **73** 2593 (2004)
32. K Morita, K Morimoto, D Kaji, T Akiyama1, S Goto, H Haba, E Ideguchi, K Katori, H Koura, H Kikunaga, H Kudo, T Ohnishi, A Ozawa, N Sato, T Suda, K Sueki, F Tokanai, T Yamaguchi, A Yoneda1, A Yoshida *J. Phys. Soc. Jpn.* **76** 045001 (2007)
33. Yu Ts Oganessian *J. Phys. G: Nucl. Part. Phys.* **34** R165 (2007)
34. R Eichler, N V Aksenov, A V Belozerov, G A Bozhikov, V I Chepigin, S N Dmitriev, R Dressler, H W Gäggeler, A V Gorshkov, M G Itkis, F Haenssler, A Laube, V Ya Lebedev, O N Malyshev, Yu Ts Oganessian, O V Petrushkin, D Piguet, A G Popeko, P Rasmussen, S V Shishkin, A A Serov, A V Shutov, A I Svirikhin, E E Tereshatov, G K Vostokin, M Wegrzecki, A V Yeremin *Angew. Chem., Int. Ed.* **47** 3262 (2008)
35. S Hofmann, D Ackermann, S Antalic, H G Burkhard, V F Comas, R Dressler, Z Gan, S Heinz, J A Heredia, F P Heßberger, J Khuyagbaatar, B Kindler, I Kojouharov, P Kuusiniemi, M Leino, B Lommel, R Mann, G Münzenberg, K Nishio, A G Popeko, S Saro, H J Schött, B Streicher, B Sulignano, J Uusitalo, M Venhart, A V Yeremin *Eur. Phys. J. A* **32** 251 (2007)
36. C M Folden III, K E Gregorich, C E Düllmann, H Mahmud, G K Pang, J M Schwantes, R Sudowe, P M Zielinski, H Nitsche, D C Hoffman *Phys. Rev. Lett.* **93** 212702 (2004)
37. C M Folden III, S L Nelson, C E Düllmann, J M Schwantes, R Sudowe, P M Zielinski, K E Gregorich, H Nitsche, D C Hoffman *Phys. Rev. C.* **73** 014611 (2006)
38. M Leino, F P Heßberger *Annu. Rev. Nucl. Part. Sci.* **54** 175 (2004)
39. R-D Herzberg *J. Phys. G: Nucl. Part. Phys.* **30** R123 (2004)
40. R-D Herzberg, P T Greenlees *Prog. Part. Nucl. Phys.* **61** 674 (2008)
41. R Smolanczuk, A Sobiczewski, in *Proceedings of the XV Nuclear Physics Divisional Conference on Low Energy Nuclear Dynamics* (Eds Yu Ts Oganessian, R Kalpakchieva, W von Oertzen) (Singapore: World Scientific, 1995) p. 313
42. S Ćwiok, J Dobaczewski, P-H Heenen, P Magierski, W Nazarewicz *Nucl. Phys. A* **611** 211 (1996)
43. K Rutz, M Bender, T Bürvenich, T Schilling, P-G Reinhard, J A Maruhn, W Greiner *Phys. Rev. C* **56** 238 (1997)
44. A T Kruppa, M Bender, W Nazarewicz, P-G Reinhard, T Vertse, S Ćwiok *Phys. Rev. C* **61** 034313 (2000)
45. M Bender, W Nazarewicz, P-G Reinhard *Phys. Lett. B* **515** 42 (2001)
46. M Bender, P Bonche, T Duguet, P-H Heenen *Nucl. Phys. A* **723** 354 (2003)
47. R Smolańczuk, J Skalski, A Sobiczewski *Phys. Rev. C* **52** 1871 (1995)
48. P Möller, J R Nix, K L Kratz *At. Data Nucl. Data Tables* **66** 131 (1997)
49. W J Swiatecki, K Siwek-Wilczynska, J Wilczynski *Acta Phys. Pol. B* **38** 1565 (2007)
50. Yu Ts Oganessian, V K Utyonkov, Yu V Lobanov, F Sh Abdullin, A N Polyakov, R N Sagaidak, I V Shirokovsky, Yu S Tsyganov, A A Voinov, G G Gulbekian, S L Bogomolov, B N Gikal, A N Mezentsev, S Iliev, V G Subbotin, A M Sukhov, K Subotic, V I Zagrebaev, G K Vostokin, M G Itkis, K J Moody, J B Patin, D A Shaughnessy, M A Stoyer, N J Stoyer, P A Wilk, J M Kenneally, J H Landrum, J F Wild, R W Lougheed *Phys. Rev. C* **74** 044602 (2006)
51. Yu Ts Oganessian, V K Utyonkov, Yu V Lobanov, F Sh Abdullin, A N Polyakov, I V Shirokovsky, Yu S Tsyganov, G G Gulbekian, S L Bogomolov, B N Gikal, A N Mezentsev, S Iliev, V G Subbotin, A M Sukhov, A A Voinov, G V Buklanov, K Subotic, V I Zagrebaev, M G Itkis, J B Patin, K J Moody, J F Wild, M A Stoyer, N J Stoyer, D A Shaughnessy, J M Kenneally, P A Wilk, R W Lougheed, R I Il'kaev, S P Vesnovskii *Phys. Rev. C* **70** 064609 (2004)
52. G Münzenberg, P Armbruster, G Berthes, H Folger, F P Heßberger, S Hofmann, K Poppensieker, W Reisdorf, B Quint, K H Schmidt, H J Schött, K Sümmerer, I Zychor, M Leino, U Gollerthan, E Hanelt *Z. Phys. A* **324** 489 (1986)
53. S Hofmann, F P Heßberger, D Ackermann, S Antalic, P Cagarda, S Ćwiok, B Kindler, J Kojouharova, B Lommel, R Mann, G Münzenberg, A G Popeko, S Saro, H J Schött, A V Yeremin *Eur. Phys. J. A* **10** 5 (2001)

54. C E Düllmann, W Brüchle, R Dressler, K Eberhardt, B Eichler, R Eichler, H W Gäggeler, T N Ginter, F Glaus, K E Gregorich, D C Hoffman, E Jäger, D T Jost, U W Kirbach, D M Lee, H Nitsche, J B Patin, V Pershina, D Piguet, Z Qin, M Schädel, B Schausten, E Schimpf, H J Schött, S Soverna, R Sudowe, P Thörle, S N Timokhin, N Trautmann, A Türler, A Vahle, G Wirth, A B Yakushev, P M Zielinski *Nature (London)* **418** 859 (2002)
55. D C Hoffman *Nucl. Phys. A* **502** 21 (1989)
56. P Möller, J R Nix, W D Myers, W J Swiatecki *At. Data Nucl. Data Tables* **59** 185 (1995)
57. I Muntian, Z Patyk, A Sobiczewski *Acta Phys. Pol. B* **32** 691 (2001)
58. S Hofmann, D Ackermann, S Antalic, V F Comas, S Heinz, J A Heredia, F P Heyberger, J Khuyagbaatar, B Kindler, I Kojouharov, M Leino, B Lommel, R Mann, K Nishio, A G Popeko, S Saro, J Uusitalo, M Venhart, A V Yeremin *GSI Annual Report 2008* in the press (2009)
59. V I Zagrebaev, W Greiner *Phys. Rev. C* **78** 34610 (2008)
60. Yu Ts Oganessian, V K Utyonkov, Yu V Lobanov, F Sh Abdullin, A N Polyakov, R N Sagaidak, I V Shirokovsky, Yu S Tsyganov, A A Voinov, A N Mezentsev, V G Subbotin, A M Sukhov, K Subotic, V I Zagrebaev, S N Dmitriev, R A Henderson, K J Moody, J M Kenneally, J H Landrum, D A Shaughnessy, M A Stoyer, N J Stoyer, P A Wilk *Phys. Rev. C* **79** 024603 (2009)
61. R Bass *Nucl. Phys. A* **231** 45 (1974)
62. P Reiter, T L Khoo, C J Lister, D Seweryniak, I Ahmad, M Alcorta, M P Carpenter, J A Cizewski, C N Davids, G Gervais, J P Greene, W F Henning, R V F Janssens, T Lauritsen, S Siem, A A Sonzogni, D Sullivan, J Uusitalo, I Wiedenhlver, N Amzal, P A Butler, A J Chewter, K Y Ding, N Fotiades, J D Fox, P T Greenlees, R D Herzberg, G D Jones, W Korten, M Leino, K Vetter *Phys. Rev. Lett.* **82** 509 (1999)
63. M Leino, R G Allatt, J F C Cocks, O Dorvaux, K Eskola, P T Greenlees, K Helariutta, P M Jones, R Julin, S Juutinen, H Kankaanpii, A Keenan, H Kettunen, P Kuusiniemi, M Muikku, P Nieminen, R D Page, P Rahkila, A Savelius, W H Trzaska, J Uusitalo *Acta Phys. Pol. B* **30** 635 (1999)
64. R D Herzberg, N Amzal, F Becker, P A Butler, A J C Chewter, J F C Cocks, O Dorvaux, K Eskola, J Gerl, P T Greenlees, N J Hammond, K Hauschild, K Helariutta, F P Heyberger, M Houry, G D Jones, P M Jones, R Julin, S Juutinen, H Kankaanpii, H Kettunen, T L Khoo, W Korten, P Kuusiniemi, Y Le Coz, M Leino, C J Lister, R Lucas, M Muikku, P Nieminen, R D Page, P Rahkila, P Reiter, Ch Schlegel, C Scholey, O Stezowski, Ch Theisen, W H Trzaska, J Uusitalo, H J Wollersheim *Phys. Rev. C* **65** 014303 (2001)
65. S Ćwiok, S Hofmann, W Nazarewicz *Nucl. Phys. A* **573** 356 (1994)
66. I Muntian, Z Patyk, A Sobiczewski *Phys. Rev. C* **60** 041302 (1999)
67. G A Lalazissis, M M Sharma, P Ring, Y K Gambhir *Nucl. Phys. A* **608** 202 (1996)
68. Z Patyk, A Sobiczewski *Nucl. Phys. A* **533** 132 (1991)
69. I Muntian, Z Patyk, A Sobiczewski *Phys. Lett. B* **500** 241 (2001)
70. A Sobiczewski, I Muntian, Z Patyk *Phys. At. Nucl.* **64** 1105 (2001)
71. A Ghiorso, K Eskola, P Eskola, M Nurmia *Phys. Rev. C* **7** 2032 (1973)
72. F R Xu, E G Zhao, R Wyss, P M Walker *Phys. Rev. Lett.* **92** 252501 (2004)
73. J-P Delaroche, M Girod, H Goutte, J Libert *Nucl. Phys. A* **771** 103 (2006)
74. S Eeckhaudt, P T Greenlees, N Amzal, J E Bastin, E Bouchez, P A Butler, A Chatillon, K Eskola, J Gerl, T Grahn, A Glrgen, R D Herzberg, F P Heyberger, A Hmrstel, P J C Ikin, G D Jones, P Jones, R Julin, S Juutinen, H Kettunen, T L Khoo, W Korten, P Kuusiniemi, Y Le Coz, M Leino, A P Leppinen, P Nieminen, J Pakarinen, J Perkowski, A Pritchard, P Reiter, P Rahkila, C Scholey, Ch Theisen, J Uusitalo, K van de Vel, J Wilson *Eur. Phys. J. A* **26** 227 (2005)
75. D Peterson, B B Back, R V F Janssens, T L Khoo, C J Lister, D Seweryniak, I Ahmad, M P Carpenter, C N Davids, A A Hecht, C L Jiang, T Lauritsen, X Wang, S Zhu, F G Kondev, A Heinz, J Qian, R Winkler, P Chowdhury, S K Tandel, U S Tandel *Phys. Rev. C* **74** 014316 (2006)
76. S K Tandel, T L Khoo, D Seweryniak, G Mukherjee, I Ahmad, B Back, R Blinstrup, M P Carpenter, J Chapman, P Chowdhury, C N Davids, A A Hecht, A Heinz, P Ikin, R V F Janssens, F G Kondev, T Lauritsen, C J Lister, E F Moore, D Peterson, P Reiter, U S Tandel, X Wang, S Zhu *Phys. Rev. Lett.* **97** 082502 (2006)
77. R D Herzberg, P T Greenlees, P A Butler, G D Jones, M Venhart, I G Darby, S Eeckhaudt, K Eskola, T Grahn, C Gray-Jones, F P Heßberger, P Jones, R Julin, S Juutinen, S Ketelhut, W Korten, M Leino, A-P Leppänen, S Moon, M Nyman, R D Page, J Pakarinen, A Pritchard, P Rahkila, J Sarén, C Scholey, A Steer, Y Sun, Ch Theisen, J Uusitalo *Nature (London)* **442** 896 (2006)
78. B Sulignano, S Heinz, F P Heßberger, S Hofmann, D Ackermann, S Antalic, B Kindler, I Kojouharov, P Kuusiniemi, B Lommel, R Mann, K Nishio, A G Popeko, S Saro, B Streicher, M Venhart, A V Yeremin *Eur. Phys. J. A* **33** 327 (2007)
79. K Blaum *Phys. Rep., Rev. Sec. Phys. Lett.* **425** 1 (2006)
80. C Weber, V-V Elomaa, R Ferrer, C Fröhlich, D Ackermann, J Äystö, G Audi, L Batist, K Blaum, M Block, A Chaudhuri, M Dworschak, S Eliseev, T Eronen, U Hager, J Hakala, F Herfurth, F P Heßberger, S Hofmann, A Jokinen, A Kankainen, H-J Kluge, K Langanke, A Martin, G Martinez-Pinedo, M Mazzocco, I D Moore, J B Neumayr, Yu N Novikov, H Penttilä, W R Plaß, A V Popov, S Rahaman, T Rauscher, C Rauth, J Rissanen, D Rodriguez, A Saastamoinen, C Scheidenberger, L Schweikhard, D M Seliverstov, T Sonoda, F-K Thielemann, P G Thirolf, G K Vorobjev *Phys. Rev. C* 78 054310 (2008)
81. C Rauth, D Ackermann, K Blaum, M Block, A Chaudhuri, Z Di, S Eliseev, R Ferrer, D Habs, F Herfurth, F P Heßberger, S Hofmann, H-J Kluge, G Maero, A Martin, G Marx, M Mukherjee, J B Neumayr, W R Plaß, S Rahaman, D Rodriguez, C Scheidenberger, L Schweikhard, P G Thirolf, G Vorobjev, C Weber *Phys. Rev. Lett.* **100** 012501 (2008)
82. G Audi, A H Wapstra, C Thibault *Nucl. Phys. A* **729** 337 (2003)
83. P Armbruster, Y K Agarwal, W Brüchle, M Brügger, J P Dufour, H Gäggeler, F P Heßberger, S Hofmann, P Lemmertz, G Münzenberg, K Poppensieker, W Reisdorf, M Schädel, K H Schmidt, J R H Schneider, W F W Schneider, K Sümmerer, D Vermeulen, G Wirth, A Ghiorso, K E Gregorich, D Lee, M Leino, K J Moody, G T Seaborg, R B Welch, P Wilmarth, S Yashita, C Frink, N Greulich, G Herrmann, U Hickmann, N Hildebrand, J V Kratz, N Trautmann, M M Fowler, D C Hoffman, W R Daniels, H R von Gunten, H Dornhöfer *Phys. Rev. Lett.* **54** 406 (1985)
84. V I Zagrebaev, M G Itkis, Yu Ts Oganessian *Phys. At. Nucl.* **66** 1033 (2003)
85. W Reisdorf, M Schädel *Z. Phys. A* **343** 47 (1992)
86. M Schädel, S Hofmann *J. Radioanal. Nucl. Chem.* **203** 283 (1996)
87. W J Świątecki, K Siwek-Wilczyńska, J Wilczyński *Phys. Rev. C* **71** 014602 (2005)
88. V I Zagrebaev *Phys. Rev. C* **64** 034606 (2001)
89. V I Zagrebaev, Y Aritomo, M G Itkis, Yu Ts Oganessian, M Ohta *Phys. Rev. C* **65** 014607 (2002)
90. I Muntian, Z Patyk, A Sobiczewski *Acta Phys. Pol. B* **34** 2141 (2003)
91. W von Oertzen *Z. Phys. A* **342** 177 (1992)
92. V V Volkov *Phys. Part. Nucl.* **35** 425 (2004)
93. S Hofmann, in *Proceedings of the XV Nuclear Physics Divisional Conference on Low Energy Nuclear Dynamics* (Eds Yu Ts Oganessian, R Kalpakchieva, W von Oertzen) (Singapore: World Scientific, 1995) p. 305
94. V Yu Denisov, S Hofmann *Phys. Rev. C* **61** 034606 (2000)
95. M G Itkis, Yu Ts Oganessian, V I Zagrebaev *Phys. Rev. C* **65** 044602 (2002)

96. J Maruhn, W Greiner *Z. Phys. A* **251** 431 (1972)
97. A Săndulescu, R K Gupta, W Scheid, W Greiner *Phys. Lett. B* **60** 225 (1976)
98. R K Gupta, C Pârvulescu, A Săndulescu, W Greiner *Z. Phys. A* **283** 217 (1977)
99. D Scharnweber, U Model, W Greiner *Phys. Rev. Lett.* **24** 601 (1970)
100. U Mosel, J Maruhn, W Greiner *Phys. Lett. B* **34** 587 (1971)
101. A Săndulescu, W Greiner *Rep. Prog. Phys.* **55** 1423 (1992)
102. A Săndulescu, R K Gupta, W Greiner, F Carstoiu, M Horoi *Int. J. Mod. Phys. E* **1** 379 (1992)
103. P Möller, A Iwamoto *Nucl. Phys. A* **575** 381 (1994)
104. A Iwamoto, P Möller, J R Nix, H Sagawa *Nucl. Phys. A* **596** 329 (1996)
105. S Misicu, W Greiner *Phys. Rev. C* **66** 044606 (2002)
106. G Fazio, G Giardina, A Lamberto, R Ruggeri, C Sacca, R Palamara, A I Muminov, A K Nasirov, U T Yakhshiev, F Hanappe, T Materna, L Stuttge *Eur. Phys. J. A* **19** 89 (2004)
107. K Nishio, S Hofmann, F P Heßberger, D Ackermann, S Antalic, V F Comas, Z Gan, S Heinz, J A Heredia, H Ikezoe, J Khuyagbaatar, B Kindler, I Kojouharov, P Kuusiniemi, B Lommel, R Mann, M Mazzocco, S Mitsuoka, Y Nagame, T Ohtsuki, A G Popeko, S Saro, H J Schött, B Sulignano, A Svirikhin, K Tsukada, K Tsuruta, A V Yeremin *Eur. Phys. J. A* **29** 281 (2006)
108. G G Adamian, N V Antonenko, W Scheid *Nucl. Phys. A* **678** 24 (2000)
109. V Yu Denisov, W Nörenberg *Eur. Phys. J. A* **15** 375 (2002)
110. Y Aritomo, T Wada, M Ohta, Y Abe *Phys. Rev. C* **59** 796 (1999)
111. G Giardina, S Hofmann, A I Muminov, A K Nasirov *Eur. Phys. J. A* **8** 205 (2000)
112. R Smolańczuk *Phys. Rev. C* **63** 044607 (2001)
113. G Fazio, G Giardina, G Mandaglio, F Hanappe, A I Muminov, A K Nasirov, W Scheid, L Stuttge *Mod. Phys. Lett. A* **20** 391 (2005)
114. G G Adamian, N V Antonenko, A S Zubov *Phys. Rev. C* **71** 34603 (2005)
115. G G Adamian, N V Antonenko *Phys. Rev. C* **72** 64617 (2005)
116. T Ichikawa, A Iwamoto, P Möller, A J Sierk *Phys. Rev. C* **71** 44608 (2005)
117. V Yu Denisov, N A Pilipenko *Phys. Rev. C* **76** 14602 (2007)
118. V I Zagrebaev, Yu Ts Oganessian, M G Itkis, W Greiner *Phys. Rev. C* **73** 031602(R) (2006)
119. S Heinz, V Comas, F P Heßberger, S Hofmann, D Ackermann, H G Burkhard, Z Gan, J Heredia, J Khuyagbaatar, B Kindler, B Lommel, R Mann, J Maurer, K Nishio, B Sulignano *Eur. Phys. J. A* **38** 227 (2008)
120. P Reiter, T L Khoo, T Lauritsen, C J Lister, D Seweryniak, A A Sonzogni, I Ahmad, N Amzal, P Bhattacharyya, P A Butler, M P Carpenter, A J Chewter, J A Cizewski, C N Davids, K Y Ding, N Fotiades, J P Greene, P T Greenlees, A Heinz, W F Henning, R -D Herzberg, R V F Janssens, G D Jones, H Kankaanpää, F G Kondev, W Korten, M Leino, S Siem, J Uusitalo, K Vetter, I Wiedenhlver *Phys. Rev. Lett.* **84** 3542 (2000)